

## EXTREME-ULTRAVIOLET JETS AND H $\alpha$ SURGES IN SOLAR MICROFLARES

JONGCHUL CHAE, JIONG QIU, HAIMIN WANG, AND PHILIP R. GOODE

Big Bear Solar Observatory, New Jersey Institute of Technology, 40386 North Shore Lane, Big Bear City, CA 92314-9672; chae@bbso.njit.edu

Received 1998 November 23; accepted 1999 January 4; published 1999 January 25

### ABSTRACT

We analyzed simultaneous EUV data from the *Transition Region and Coronal Explorer* and H $\alpha$  data from Big Bear Solar Observatory. In the active region studied, we found several EUV jets that repeatedly occurred where pre-existing magnetic flux was “canceled” by newly emerging flux of opposite polarity. The jets look like *Yohkoh* soft X-ray jets, but are smaller and shorter lived than X-ray jets. They have a typical size of 4000–10,000 km, a transverse velocity of 50–100 km s<sup>-1</sup>, and a lifetime of 2–4 minutes. Each of the jets was ejected from a looplike bright EUV emission patch at the moment that the patch reached its peak emission. We also found dark H $\alpha$  surges that are correlated with these jets. A careful comparison, however, revealed that the H $\alpha$  surges are not cospatial with the EUV jets. Instead, the EUV jets are identified with bright jetlike features in the H $\alpha$  line center. Our results support a picture in which H $\alpha$  surges and EUV jets represent different kinds of plasma ejection—cool and hot plasma ejections along different field lines—which must be dynamically connected to each other. We emphasize the importance of observed flux cancellation and a small erupting filament in understanding the acceleration mechanisms of EUV jets and H $\alpha$  surges.

*Subject headings:* MHD — Sun: chromosphere — Sun: flares — Sun: magnetic fields — Sun: UV radiation

### 1. INTRODUCTION

Dynamical phenomena associated with solar flares, which include H $\alpha$  surges (Roy 1973), erupting filaments, EUV jets or surges (Schmahl 1981), and X-ray jets (Shibata et al. 1992), have been extensively studied at various wavelengths. Of particular interest have been efforts to reveal the relationship between cool plasma material, represented by H $\alpha$  surges, and hot plasma material, represented by brightenings or jets in EUV and X-ray. From a comparison of *Skylab* X-ray images and H $\alpha$  surges, Rust, Web, & Maccombie (1977) found that few H $\alpha$  surges were coincident with noticeable changes in X-ray emission. Further, they found that the time interval between X-ray images and H $\alpha$  images was so long as to call into question the meaning of the occasional apparent coincidences. Schmahl (1981) searched for H $\alpha$  surgelike structures in EUV (which he called EUV surges) using the Harvard spectroheliometer on the Apollo Telescope Mount. EUV surges, however, appeared in emission—unlike H $\alpha$  surges. He showed that most EUV surges are associated with flares and found an example of an EUV surge that appeared to occur cospatially and simultaneously with the H $\alpha$  surge. Schmieder et al. (1988)’s comparison of H $\alpha$  surges with UV and X-ray data obtained from the *Solar Maximum Mission* supported the idea that H $\alpha$  surges are spatially correlated with UV and X-ray emission. A similar result was obtained by Švestka, Fárník, & Tang (1990). The surge they studied was bright in H $\alpha$ . Shibata et al. (1992) discovered X-ray jets using the *Yohkoh* Soft X-ray Telescope and presented an example of an X-ray jet that is nearly cospatial with an H $\alpha$  surge. Schmieder, Golub, & Antiochos (1994) also found a jetlike X-ray emission thread that overlies the brightest thread of H $\alpha$  emission in an H $\alpha$  surge. Recently, however, Canfield et al. (1996) reported that X-ray jets are not cospatial with H $\alpha$  surges even though they are associated with each other. In summary, most of the previous studies seem to support that H $\alpha$  surges are associated with EUV/X-ray brightening and jets, but the temporal and spatial relationship between them is still not clear. In all probability, the ambiguity is primarily due to the limited spatial and temporal resolution of the past experiments. In this Letter, we present observational results based on

*Transition Region and Coronal Explorer (TRACE)* EUV and Big Bear Solar Observatory (BBSO) H $\alpha$  data that elucidate the physical relationship between cool plasma and hot plasma ejections. Our key advantage over previous researchers is the excellent spatial (1”) and temporal (30–60 s) resolution of both *TRACE* and BBSO observations.

### 2. OBSERVATIONS AND DATA PROCESSING

Simultaneous observations by *TRACE* and BBSO were made of NOAA Active Region 8264 on 1998 July 9 from 16:00 to 23:00 UT. At the time of observations, the active region was located at a disk position 550” west and 243” north from disk center. The *TRACE* observing sequence included all available filters, but we present only the results based on Fe XII  $\lambda$ 195 images which were gathered at a 1 minute cadence. The spatial resolution of *TRACE* observations is 1”, which is implied by its pixel size of 0”.5. Since the *TRACE* satellite follows a polar orbit, the cosmic-ray-type noise due to the energetic particles trapped by the terrestrial polar magnetic fields is annoying in EUV data. We removed cosmic-ray-type defects using the principle of ring-filtering detection and maximum entropy smoothing.

The BBSO observations were composed of longitudinal videomagnetograms and H $\alpha$  filtergrams. The magnetograms have a spatial resolution of 2”, a temporal resolution of 1 minute, and a sensitivity of 10 G. The temporal resolution of the H $\alpha$  data is 30 s, and the spatial resolution is estimated to be 1”–1”.5. In order to reveal small-scale H $\alpha$  features better, we have enhanced the images using the maximum entropy deconvolution algorithm developed by Chae et al. (1998c). The comparison with raw images showed that the enhanced images did not introduce any significant artifacts that can affect our results. Spatial co-alignment between EUV and H $\alpha$  data were done by first co-aligning H $\alpha$  data and *TRACE* white-light data based on commonly visible spots. Then, Fe XII  $\lambda$ 195 images and white-light images were co-aligned by taking into account the small difference between the pointings in the two kinds of data (courtesy of R. Shine). According to our experiments, the accuracy in the co-alignments of EUV data and H $\alpha$  data is mainly

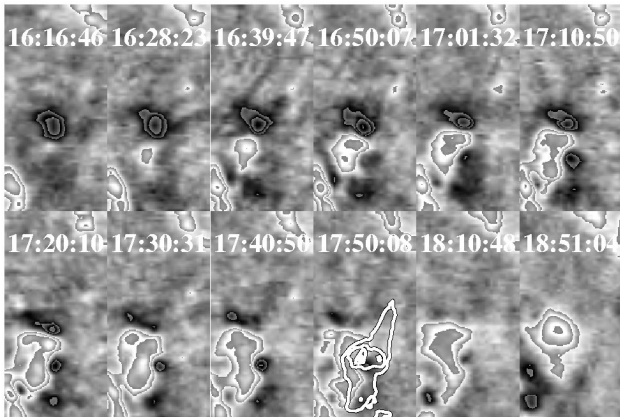


FIG. 1.—Time series of BBSO line-of-sight magnetograms. The gray-scale discontinuities represent the flux density levels of 50, 100, 200  $\text{Mx cm}^{-2}$  and so on. For comparison, the intensity contours of Fe XII  $\lambda 195$  data obtained at 17:50:56 UT were superposed on the magnetogram taken at the same time.

limited by the spatial resolution and is estimated to be better than  $2''$ .

### 3. RESULTS

NOAA AR 8264 was in its decaying phase at the time of our observations, and, not surprisingly, it did not produce any major flares. But it continually produced many transient brightenings recorded in H $\alpha$  and EUV data. BBSO magnetograms show that most of these brightenings were associated with magnetic flux “cancellation.” The jets we are going to describe occurred in a small emerging flux region. Figure 1 shows the time evolution of the flux distribution at this region during the period from 16:00 to 19:00 UT. As seen from the figure, the pre-existing magnetic flux was continually canceled and eventually replenished by newly emerging flux of the opposite polarity. The jets occurred around 17:50 UT, when the pre-existing negative background magnetic flux was canceled by the emerging flux. This indicates that the jets may have resulted from the interaction between pre-existing open (or large) loops and newly emerging small loops. Note from the figure that the jets were cospatial with the flux cancellation. The rate of flux loss due to magnetic cancellation can be estimated by measuring the amount of negative flux as a function of time. We obtained a value of  $7 \times 10^{14} \text{ Mx s}^{-1}$  for the average flux loss rate during the period 17:00–18:00 UT. This value is 1 order of magnitude larger than what was found in the case of the quiet-Sun flux cancellations which accompany UV explosive events (Chae et al. 1998a).

Figures 2 and 3 show some of the transient brightenings seen in Fe XII  $\lambda 195$  and H $\alpha$  images, respectively. We examined the importance of these brightenings in X-ray and H $\alpha$  in the context of *GOES-9* data and the area of H $\alpha$  brightening. In this context, the brightenings turn out to be very weak subflares and may be called microflares. Figure 2 shows four EUV jets identified during a 16 minute period. As seen from the figure, both the transient brightenings and the jets are spatially recurrent. Interestingly, double jets are visible at 17:52:56 UT and may be a superposition of jets 2 and 3. The figure also shows that these jets are strongly associated with the transient brightenings—that is, jets are ejected from bright EUV emission patches at instants of emission peak. Combined with the fact that this

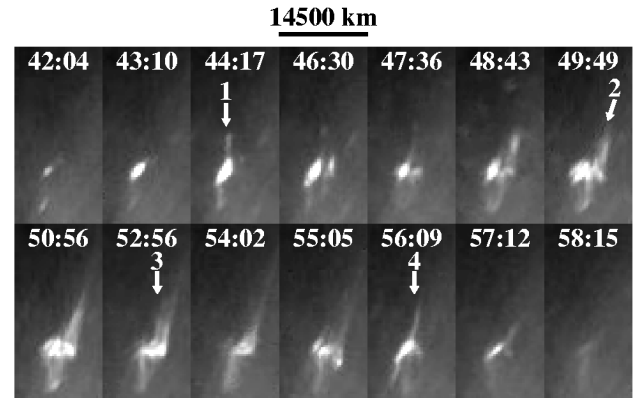


FIG. 2.—Time sequence of Fe XII  $\lambda 195$  images taken between 17:42:04 and 17:58:15 UT. The vertical arrows represent the identified EUV jets.

region was undergoing flux cancellation, this association supports the picture that both the jets and the microflares may be a result of magnetic reconnection. Without accounting for perspective, the lengths of these jets range from 4000 to 10,000 km. The jets are visible in the Fe XII  $\lambda 195$  images only for a short time—2 to 4 minutes. We cannot examine the trajectory of each jet in detail because they are weakly visible in our data and our temporal resolution is only adequate. Nonetheless, we roughly estimate the transverse velocities to be 50–100  $\text{km s}^{-1}$  within an uncertainty of a factor of 2 by assuming that it takes 1–2 minutes to reach the aforementioned lengths.

Figure 3 shows a time sequence of H $\alpha$  center-line data taken at the same position and nearly at the same times as the EUV data presented in Figure 2. Our comparison of H $\alpha$  data and EUV data reveals that the H $\alpha$  counterpart to a EUV jet is a bright H $\alpha$  feature seen in the H $\alpha$  center, as indicated by the arrows. Note that bright feature 1 seen at 17:44:24 UT has the same location and morphology as the EUV jet/brightening seen at 17:44:17 UT in Figure 2. An emission blob begins to be visible at the northern part of the bright emission patch at 17:39:54 UT, begins to move northward, and reaches its maximal displacement length of about 4000 km at 17:42:54 UT. The transverse velocity of this H $\alpha$  jet is estimated to be 30  $\text{km s}^{-1}$ . It remains visible for more than 10 minutes, unlike the corresponding EUV jet. After 17:47:54 UT, the shape of the jet changes from its initial discrete blob structure to a continuous linear structure. The next jet, jet 2, also displays a bright blob when it starts at 17:47:54 UT, but it soon changes into a continuous linear structure with a length of about 4500 km. Thus, its transverse velocity is estimated to be about 75  $\text{km s}^{-1}$ .

Figure 3 also reveals two dark H $\alpha$  surges, labelled A and B. They are correlated with the brightenings and the jets but are not cospatial with them, indicating that surges are distinct from EUV jets. Each of the surges is located on the right side of the associated bright H $\alpha$  jet in parallel to it. We find that the contrast of the surge A increases with time, reaching the peak around 17:50:54 UT when jet 1 is accelerated. After 17:50:54 UT, the surge begins to fade at its base. This may be due to the Doppler brightening caused by the upward motion. Half an hour later, at 18:30 UT, the surge material falls back as we find from the off-band H $\alpha$  data at the blue and red wings. The other surge, B, displays similar behavior. It is first visible at 17:50:54 UT. Its contrast and its width increase rapidly

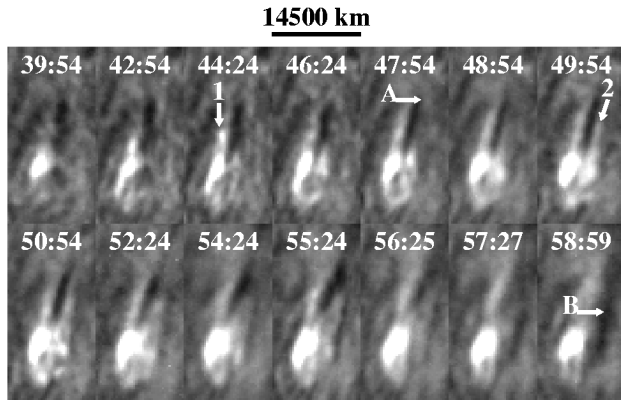


FIG. 3.—Time sequence of  $H\alpha$  center-line images taken between 17:39:54 and 17:58:59 UT. The vertical arrows (1 and 2) represent the positions of the identified  $H\alpha$  jets, and the horizontal arrows (A and B) indicate dark surges.

around 17:57:59 UT. Half an hour later, it is still visible in line center and is moving upward, as seen from the blueshift manifest in the off-band data.

Interestingly, in addition to  $H\alpha$  jets and surges, we find another kind of dynamical  $H\alpha$  feature associated with the microflares: a small erupting filament. This feature is clearly visible in the blue off-band data presented in Figure 4. The characteristics of the wavelength-dependent contrast and the pseudo-Dopplergram indicate that it is mostly blueshifted, which is the reason that we regard this feature as a small erupting filament. The darkest contrast is found at a wavelength between  $-0.75$  and  $-0.50$  Å, so the line-of-sight velocity is estimated to be about  $20$ – $30$  km  $s^{-1}$ . We want to mention two observational characteristics that may be important in understanding the physical nature of this filament. First, the blueshifted part of the filament follows the magnetic neutral line formed by the encounter of the pre-existing negative flux and newly emerging positive flux. In particular, the largest blueshift is found precisely at the flux-canceling position. The other thing is that this erupting filament event precedes EUV microflares and jets. These facts suggest that the erupting filament may be a direct result of the physical process that leads to the observed flux cancellation and may be a cause of the microflares and jets. It would be very interesting to investigate the possible relations of this kind of filament to microflares, jets, and surges by examining the temporal evolution of the filament. Unfortunately, the present data set is not adequate for such detailed study, since only a few spectral scans were made at large time intervals during the observing day.

#### 4. DISCUSSION

Our results show that the *TRACE* EUV jets studied here are very similar to the *Yohkoh* X-ray jets in shape, velocity, and in the characteristic of their association with microflares, except for the fact that the EUV jets are much smaller ( $0.4$ – $1 \times 10^4$  km) and shorter lived (a few minutes) than X-ray jets, which have sizes from a few times  $10^4$  to  $4 \times 10^5$  km and lifetimes from 100 to 16,000 s (Shimojo et al. 1996). Therefore, EUV jets are likely to have the same physical origin as X-ray jets and to represent the small-scale tail of the spectrum of X-ray jet characteristics. Further studies of the EUV jets using *TRACE* observations will extend our knowledge of large-scale magnetic reconnection events, as learned from the *Yohkoh* ex-

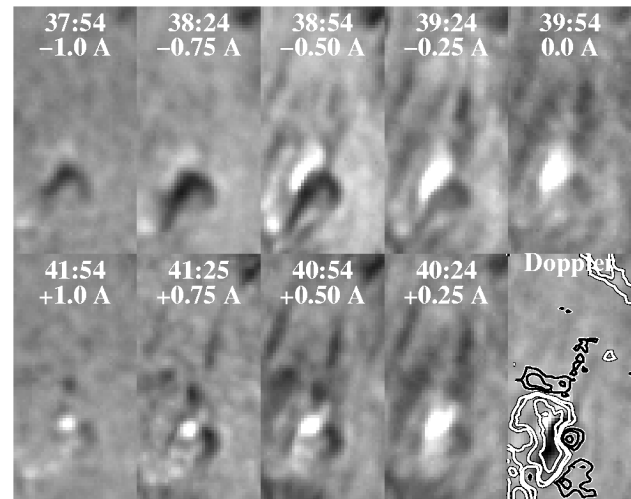


FIG. 4.—Set of  $H\alpha$  spectral scan data taken around 17:40 UT. The Dopplergram has been constructed by subtracting  $+0.5$  Å image from  $-0.5$  Å image so that dark features usually represent blueshifted ones. The contours superposed on the Dopplergram represent the magnetogram taken at the same time with the flux density levels of  $\pm 25$ , 50, and 100 G, respectively.

periments, to smaller scale magnetic reconnection events, which are evidenced by recent observations (Dere 1994; Innes et al. 1997; Chae et al. 1998a, 1998b).

Our results also show that EUV jets and  $H\alpha$  surges are different kinds of plasma ejection. They are not cospatial when spatially ( $1''$ ) well resolved, even though they appear to be strongly correlated with each other. This implies that EUV jets and  $H\alpha$  surges represent hot and cool plasma ejections along different field lines, but they must be dynamically connected to each other, supporting the finding of Canfield et al. (1996). On the other hand, we were able to find  $H\alpha$  jets that are distinct from  $H\alpha$  surges and are exactly cospatial and simultaneous with the EUV jets. The  $H\alpha$  jets appear in emission in the  $H\alpha$  center line. This fact may explain why previous authors often observed “bright  $H\alpha$  surges” (Schmahl 1981; Švestka et al. 1990) or “bright threads of  $H\alpha$  surges” (Schmieder et al. 1994), which appear to be the  $H\alpha$  counterpart of EUV or X-ray jets.

How are EUV jets and  $H\alpha$  surges accelerated? First of all, our observations do not support the pressure-driven model (e.g., Steinolfson, Schmahl, & Wu 1979), confirming Schmieder et al. (1994)’s conclusion. We can not find any evidence of high-pressure regions at the footpoints of surges. The flaring sites that may have high pressure are at the footpoints of EUV jets, but not at those of surges.  $H\alpha$  surges, therefore, should be accelerated by the Lorentz force. Based on two-dimensional numerical simulations, Yokoyama & Shibata (1996) successfully showed that not only hot plasma but also cool plasma can be accelerated by magnetic reconnection driven by emerging flux. According to their model, X-ray/EUV jets are hot reconnection jets that are accelerated by the tensile strength of the reconnected field lines and  $H\alpha$  surges are cool jets that are ejected by the sling-shot effect due to reconnection, which produces a whiplike motion. They found that cool jets and hot jets are ejected side by side with each other. Our observational results appear to be consistent with this model. However, it is not certain how the model can explain the observed flux cancellation and the small erupting filament which are associated with the EUV jets and  $H\alpha$  surges.

Flux cancellation is rarely observed in major flares such as two-ribbon flares but is frequent in microflares, so that it may represent magnetic reconnection occurring in the lower altitude. It is our impression that the physical process that leads to the observed "flux cancellation" may be different from that producing the microflares and jets since flux cancellation was already taking place before microflares occurred. Wang & Shi (1993) realized the same problem from their observations and suggested that there should be at least two kinds of magnetic reconnection: one kind leading to flux cancellation and the other kind directly responsible for flares. Quite recently, Chae (1999) proposed a schematic two-step reconnection model to explain the close correlations found among flux cancellation, chromospheric upflow events, and UV explosive events found in the quiet Sun (Chae et al. 1998a, 1998b). According to the model, flux cancellation is a direct result of slow magnetic reconnection occurring in the lower atmosphere. The slow mag-

netic reconnection forms isolated magnetic islands that are eventually ejected and collide with the overlying field lines driving the secondary fast reconnection in the upper atmosphere. It appears that the small erupting filament we observed is a direct result of the slow magnetic reconnection inferred from observed flux cancellation. We expect more observational and theoretical work to be done for a consistent understanding of all the associated phenomena we observed: flux emergence, flux cancellation, erupting filaments, EUV transient brightenings, EUV/H $\alpha$  jets, and H $\alpha$  surges.

We would like to thank the observing staff at BBSO for their support in obtaining the data and the *TRACE* team for providing very nice EUV/UV data. This work is partially supported by NSF under grant ATM-97-14796 and NASA under grants NAG5-4919, NAG5-7349, and NAG5-7350 to BBSO.

#### REFERENCES

- Canfield, R. C., Peardon, K. P., Leka, K. D., Shibata, K., Yokoyama, T., & Shimojo, M. 1996, *ApJ*, 464, 1016
- Chae, J. 1999, in *ASP Conf. Ser.*, 19th NSO/SP International Workshop on High-Resolution Solar Physics: Theory, Observations, and Techniques, ed. T. Rimmele, K. S. Balasubramaniam, & R. Radick (San Francisco: ASP), in press
- Chae, J., Wang, H., Lee, C.-Y., Goode, P. R., & Schühle, U. 1998a, *ApJ*, 497, L109
- . 1998b, *ApJ*, 504, L123
- Chae, J., Yun, H. S., Sakurai, T., & Ichimoto, K. 1998c, *Sol. Phys.*, 183, 245
- Dere, K. P. 1994, *Adv. Space Res.*, 14(4), 13
- Innes, D. E., Inhester, B., Axford, W. I., & Wilhelm, K. 1997, *Nature*, 386, 811
- Roy, J. R. 1973, *Sol. Phys.*, 32, 139
- Rust, D. M., Webb, D. F., & McCombie, D. W. 1977, *Sol. Phys.*, 54, 53
- Schmahl, E. J. 1981, *Sol. Phys.*, 69, 135
- Schmieder, B., Golub, L., & Antiochos, S. K. 1994, *ApJ*, 425, 326
- Schmieder, B., Simnett, G. M., Tandberg-Hanssen, E., & Mein, P. 1988, *A&A*, 201, 327
- Shibata, K., et al. 1992, *PASJ*, 44, L173
- Shimojo, M., Hashimoto, S., Shibata, K., Hirayama, T., Hudson, H. S., & Acton, L. W. 1996, *PASJ*, 48, 123
- Steinolfson, R. S., Schmahl, E. J., & Wu, S. T. 1979, *Sol. Phys.*, 63, 187
- Švestka, Z., Fárnik, F., & Tang, F. 1990, *Sol. Phys.*, 127, 149
- Wang, J., & Shi, Z. 1993, *Sol. Phys.*, 143, 119
- Yokoyama, T., & Shibata, K. 1996, *PASJ*, 48, 353